The formation of vault-tubes: a dynamic interaction between vaults and vault PARP

Arend van Zon[1], Marieke H. Mossink[1], Martijn Schoester[1], Adriaan B. Houtsmuller[2], George L. Scheffer[3], Rik J. Scheper[3], Pieter Sonneveld[1] and Erik A. C. Wiemer[4,*]

[1]Department of Hematology, Erasmus Medical Center, PO Box 1738, 3000 DR Rotterdam, The Netherlands
[2]Department of Pathology, Erasmus Medical Center/Josephine Nefkens Institute, PO Box 1738, 3000 DR Rotterdam, The Netherlands
[3]Department of Pathology, Free University Medical Center, PO Box 7057, 1007 MB Amsterdam, The Netherlands
[4]Department of Medical Oncology, Erasmus Medical Center/Josephine Nefkens Institute, PO Box 1738, 3000 DR Rotterdam, The Netherlands
*Author for correspondence (e-mail: e.wiemer@erasmusmc.nl)

Accepted 7 July 2003
Journal of Cell Science 116, 4391-4400 © 2003 The Company of Biologists Ltd
doi:10.1242/jcs.00749

Summary

Vaults are barrel-shaped cytoplasmic ribonucleoprotein particles that are composed of a major vault protein (MVP), two minor vault proteins [telomerase-associated protein 1 (TEP1), vault poly(ADP-ribose) polymerase (VPARP)] and small untranslated RNA molecules. Not all expressed TEP1 and VPARP in cells is bound to vaults. TEP1 is known to associate with the telomerase complex, whereas VPARP is also present in the nuclear matrix and in cytoplasmic clusters (VPARP-rods). We examined the subcellular localization and the dynamics of the vault complex in a non-small cell lung cancer cell line expressing MVP tagged with green fluorescent protein. Using quantitative fluorescence recovery after photobleaching (FRAP) it was shown that vaults move temperature independently by diffusion. However, incubation at room temperature (21°C) resulted in the formation of distinct tube-like structures in the cytoplasm. Raising the temperature could reverse this process. When the vault-tubes were formed, there were fewer or no VPARP-rods present in the cytoplasm, suggesting an incorporation of the VPARP into the vault-tubes. MVP molecules have to interact with each other via their coiled-coil domain in order to form vault-tubes. Furthermore, the stability of microtubules influenced the efficiency of vault-tube formation at 21°C. The dynamics and structure of the tubes were examined using confocal microscopy. Our data indicate a direct and dynamic relationship between vaults and VPARP, providing further clues to unravel the function of vaults.

Key words: MVP, VPARP, TEP1, vRNA, Vault complex

Introduction

Vaults are the largest ribonucleoprotein particles described to date. They were named for their typical lobular morphology, which is reminiscent of the vaulted ceilings in cathedrals (Kedersha and Rome, 1986). Mammalian vaults are composed of multiple copies of three different proteins (p240, p193 and p100) and several small untranslated RNA molecules of 88-141 bases. The vault components assemble into a 13 MDa hollow barrel-like structure of about 35×65 nm (Kong et al., 2000; Kong et al., 1999) that is predominantly localized in the cytoplasm. Nevertheless, a small part (~5%) of major vault protein (MVP) is consistently associated with the nucleus (Abbondanza et al., 1998; Chugani et al., 1993). Although the cellular function of vaults is still unknown, their subcellular localization and distinct morphology point to a role for vaults in intracellular, particularly nucleo-cytoplasmic, transport (Abbondanza et al., 1998; Chugani et al., 1993; Hamill and Suprenant, 1997; Herrmann et al., 1999; Herrmann et al., 1996; Kitazono et al., 2001; Kitazono et al., 1999; Li et al., 1999). Vaults are frequently upregulated in multidrug-resistant cell lines and tumors of different histogenetic origin. Furthermore, they are highly expressed in tissues exposed to xenobiotics. It has been suggested that vaults function in cellular detoxification processes by transporting harmful agents away from their cellular targets (for a review, see Scheffer et al., 2000).

The p100 subunit or MVP constitutes over 70% of the molecular mass of vaults and is the main determinant of the vault structure (Stephen et al., 2001). Interaction between MVP molecules is mediated by the coiled-coil domain present in the C-terminal half of the protein (van Zon et al., 2002). The p240 protein is identical to the telomerase-associated protein 1 (TEP1) and appears to be shared between at least two ribonucleoprotein complexes, i.e. vaults and the telomerase complex (Harrington et al., 1997; Kickhoefer et al., 1999b). TEP1 is capable of binding vault RNA and is required for the overall stability and stable association of the vault RNA with the vault complex (Kickhoefer et al., 2001). The vault RNA itself is thought to be a functional vault component rather than a structural one (Kedersha et al., 1991; Kong et al., 2000; van Zon et al., 2001). The p193 protein or VPARP [vault poly(ADP-ribose) polymerase] exhibits a poly(ADP-ribose) polymerase activity and can poly(ADP-ribosylate) MVP and, to a lesser extent, itself (Kickhoefer et al., 1999a). Whether there are other substrates for VPARP is presently unknown. VPARP is a member of a growing family of enzymes, which include PARP-1 and tankyrase (D'Amours et al., 1999; Smith, 2001). Although having a similarity of 29-60% between their

PARP domains, the PARP proteins in general do not resemble each other outside the PARP domain, suggesting they have separate cellular functions. Unique features of VPARP are a BRCA1 C-terminus (BRCT) domain (aa 1-94) and an inter-α-inhibitor domain (aa 616-1195); both domains may be involved in protein-protein interactions. The C-terminus of VPARP (aa 1562-1724) has been shown to associate with the N-terminal part of MVP (Kickhoefer et al., 1999a; van Zon et al., 2002). Immunofluorescence and biochemical fractionation studies clearly indicate that not all VPARP is bound to vaults; VPARP is also present in the nuclear matrix and in distinct cytoplasmic clusters (Kickhoefer et al., 1999a; Schroeijers et al., 2000) (this manuscript). It is not clear whether VPARP fulfils separate functions – unrelated to vault function – in its non-vault-associated form.

Although the vault components and structure have been characterized in detail, little is known about the intracellular distribution and mobility of vaults in vivo and their relation to non-vault-associated minor vault proteins. To visualize the vault complex, we fused green fluorescent protein (GFP) to the MVP. Bleaching experiments showed that vaults in the cytoplasm are freely mobile and move by diffusion. However, incubation of cells at 21°C resulted in the formation of highly regular and dynamic vault-tubes. We present evidence for a role of the cytoplasmic non-vault-associated VPARP-rods in vault-tube formation.

Materials and Methods

Cell lines and culture conditions

The following human cell lines were used: the cervix epitheloid carcinoma cell line HeLa, the non-small cell lung carcinoma cell line SW1573 and its doxorubicin-selected multidrug resistant (MDR) variant SW1573/2R120 (Kuiper et al., 1990). The cell line SW1573 was transfected with a construct encoding a C-terminal GFP-tagged MVP or truncated MVP (aa 1-706); the resulting cell lines were named SW1573/MVP-GFP and SW1573/MVP706-GFP. All cell lines were maintained in Dulbecco's Modified Eagle's Medium (DMEM) (Life Technologies, Paisley, UK), supplemented with 10% (vol/vol) fetal calf serum, 1 mM pyruvate, 100 U/ml penicillin and 100 μg/ml streptomycin (Life Technologies) at 37°C under an atmosphere containing 5% CO_2. The drug-resistant cell line, SW1573/2R120, was cultured in the presence of 120 nM doxorubicin. The transfected cell lines were cultured in medium containing 200 μg/ml of G-418 (Life Technologies).

GFP-tagged MVP, MVP deletion constructs and transfection

An expression construct was generated by cloning the full-length human MVP cDNA in frame to the 5′ end of the enhanced GFP coding sequence. Full-length MVP cDNA cloned in pBS-KSII was used as a PCR template with the following primers: forward primer 5′-CCC-AAGCTTGTCACCATGGCAACTGAAGAG and reverse primer 5′-CGGGATCCCGCAGTACAGGCACCACGTGG introducing a *Hin*dIII and *Bam*HI restriction site to facilitate cloning in pEGFP-N1 (Clonetech laboratories Inc., Palo Alto, CA). The PCR conditions were as follows: 95°C for 2 minutes, then 35 cycles of 95°C for 30 seconds, 58°C for 1 minute and 72°C for 3 minutes followed by 72°C for 10 minutes using *Pfu* DNA polymerase (Stratagene, La Jolla, CA). The amplified DNA fragments were size fractionated by agarose gel electrophoresis, isolated and extracted from agarose gel and ligated into pCR®-Blunt (Invitrogen, Carlsbad, CA). The MVP fragments were released from the vector by digestion with the appropriate restriction enzymes and subsequently cloned into the GFP expression vector. A cDNA fragment of human MVP encoding amino acids 1-706 was amplified by standard PCR using 5′-CCCAAGCTTGTC-ACCATGGCAACTGAAGAG as a forward primer and 5′-CCGG-ATCCTCCAAAAGTTCCTTGCGAGC as reverse primer. To prevent PCR artifacts we used *Pfu* polymerase combined with a low number of PCR cycli. Amplified fragments containing appropriate restriction sites were cloned in pZeroblunt (Invitrogen). Subsequently, the *Hin*dIII-*Bam*HI MVP fragments were cloned in the *Hin*dIII- and *Bam*HI-digested and dephosphorylated vector pEGFP-N1 (Clontech). The resulting expression plasmid MVP706-GFP expresses GFP fused to a MVP truncated at its C-terminal end. Transfection of the SW1573 cell line was performed by calcium-phosphate precipitation as described previously (Parker and Stark, 1979). Approximately 48 hours after transfection, transfectants were selected by the addition of 800 μg/ml of G-418. The G-418-resistant and GFP-expressing cells were isolated using a fluorescence-activated cell sorter (FACS) and cultured in the presence of 200 μg/ml G-418.

Antibodies

The mouse monoclonal anti-VPARP (mAb p193-4), mouse monoclonal anti-MVP (LRP-56) and the rabbit polyclonal anti-MVP were generated as described previously (Schroeijers et al., 2000). The mouse monoclonal anti-β-tubulin and a species-specific isotype antibody were purchased from the Sigma-Aldrich Corporation (St Louis, MO), and the rabbit polyclonal anti-GFP was purchased at Clontech Laboratories Inc. Species-specific anti-Ig antibodies conjugated to tetramethyl rhodamine isothiocyanate (TRITC), fluorescein isothiocyanate (FITC) or horseradish peroxidase (HRP) were obtained from Jackson ImmunoResearch Laboratories Inc. (West Grove, PA).

Immunoprecipitation, cell fractionation, SDS-PAGE and western blot analysis

Antibodies were coupled to Protein A-Sepharose beads (Amersham Pharmacia Biotech, Uppsala, Sweden) according to the recommendations of the manufacturer. Immunoprecipitations from protein lysates prepared in lysis buffer [50 mM Tris-Cl pH 7.4, 1.5 mM $MgCl_2$, 75 mM NaCl, 0.5% (vol/vol) Nonidet P-40], supplemented with a proteinase inhibitor cocktail (Complete™, Roche, Mannheim, FRG) were carried out for 2 hours at 4°C. Subsequently, the beads were washed with lysis buffer and twice with PBS, after which the beads were suspended in protein sample buffer. Immunoprecipitated proteins were analyzed by SDS-PAGE and western blotting. A cellular fraction, enriched for vaults, was prepared as follows: cells were harvested and resuspended in lysis buffer supplemented with a proteinase inhibitor cocktail. All subsequent steps were performed at 4°C. The cell lysate was incubated on ice for 5 minutes and cleared from nuclei by centrifugation for 20 minutes at 20,000 ***g***. The supernatant was centrifuged at 100,000 ***g*** for 90 minutes, resulting in a pellet fraction enriched for vaults. Equal portions of the resulting supernatant and pellet fraction were subjected to SDS-PAGE, after which the size-fractionated proteins were transferred to nitrocellulose. The remaining protein binding sites on western blots were blocked by Tris buffered saline/Tween 20 (TBST) [50 mM Tris-Cl pH 7.5, 100 mM NaCl, 0.05% (vol/vol) Tween 20] containing 5% (wt/vol) non-fat dry milk (Bio-Rad Laboratories, Hercules, CA). Consecutively, primary and secondary antibody incubations were carried out in the same buffer. Immune-complexes were detected using the BM Chemiluminescence Blotting Substrate (POD) kit (Roche, Mannheim, FRG) and visualized on Hyperfilm™ ECL™ (Amersham Pharmacia Biotech).

Fluorescence microscopy

Cells were grown on poly-L-lysine-coated coverslips, after which they

were fixed with 3% (vol/vol) formaldehyde in PBS for 20 minutes. Subsequently, the cells were permeabilized by 1% (vol/vol) Triton-X100 in PBS for 5 minutes. The remaining protein binding sites were blocked with 1% (wt/vol) BSA in PBS for 30 minutes. Primary and secondary antibody incubations were performed in the same buffer for 60 minutes at room temperature (21°C) using 25 μg/ml p193.4 mAb, 10 μg/ml LRP-56 and FITC- or TRITC-conjugated goat anti-mouse Ig in a dilution as recommended by the manufacturer. Between each antibody incubation step the coverslips were washed six times in PBS. Coverslips were mounted on microscope slides in anti-fade [4% (wt/vol) *n*-propyl gallate in glycerol] or VectaShield mounting medium (Vector Laboratories Inc., Burlingame, CA). The fluorescent staining pattern was studied using a Leica DMRXA microscope and pictures were created using Leica QFish version V 2.3e.

Confocal microscopy and fluorescence recovery after photobleaching (FRAP)

A Zeiss (Jena, FRG) confocal laser-scanning microscope (CLSM) equipped with a thermostatted stage was used for confocal microscopy and FRAP experiments. Excitation illumination was by an argon ion laser at 488 nm. Images were taken at a lateral resolution of 102 nm using a 40× 1.3 n.a. objective. To determine cytoplasmic mobility of vaults, a strip 2 μm wide spanning the width of the cytoplasm was bleached by a short bleach pulse (200 milliseconds) at relatively high laser intensity. Subsequently, fluorescence intensity was monitored within the bleached strip at intervals of 100 milliseconds. The relative fluorescence intensity data was then fitted to diffusion curves obtained by Monte Carlo computer simulation of diffusion, immobile fraction and binding time in an ellipsoid representing the cytoplasm with a sphere inside where the molecules cannot go (representing the nucleus) (Hoogstraten et al., 2002). To determine the dynamics of protein associated with vault-tubes, the laser beam was focused in the center of a vault-tube and the region in the beam was bleached for 4 seconds (at relatively low laser power). Fluorescence redistribution was followed in time.

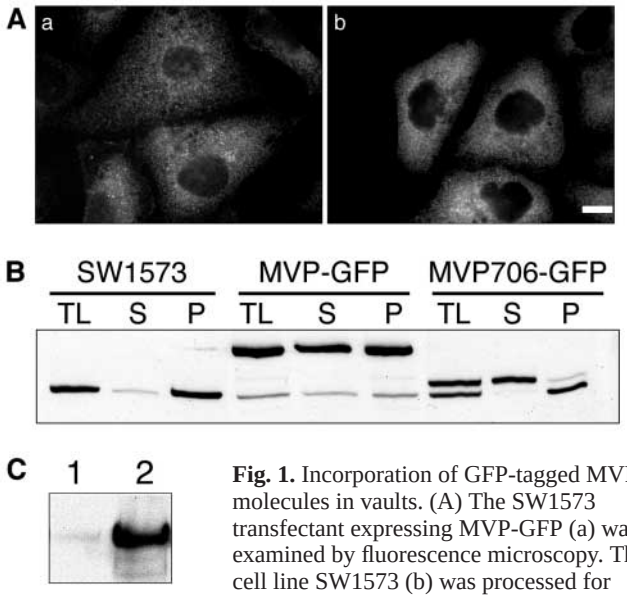

Fig. 1. Incorporation of GFP-tagged MVP molecules in vaults. (A) The SW1573 transfectant expressing MVP-GFP (a) was examined by fluorescence microscopy. The cell line SW1573 (b) was processed for indirect immunofluorescence and stained with anti-MVP (LRP-56). Bar, 10 μm. (B) Vault particles were pelleted from a total cell lysate (TL) of SW1573, SW1573/MVP-GFP transfectants and SW1573 transfectants expressing a GFP-tagged truncated MVP (SW1573/MVP706-GFP) by a 100,000 ***g*** centrifugation step. Immunoblotting using rabbit polyclonal anti-MVP was performed to determine the presence of MVP and the GFP-fusion proteins in the resulting pellet (P) and supernatant (S) fractions. Note that SW1573/MVP-GFP and SW1573/MVP706-GFP show two bands, representing endogenous (lower band) and GFP-tagged MVP or truncated MVP (upper band). (C) Immunoblot analysis showing the presence of the minor vault protein VPARP in immunoprecipitates obtained from MVP-GFP transfectants using anti-GFP (lane 2). Lane 1 contains control immunoprecipitates in which a polyclonal rabbit pre-immune serum was used.

Results

GFP-tagged MVP proteins are incorporated into intact vaults

To investigate the subcellular distribution and dynamics of the vault complex, GFP was fused to the C-terminus (MVP-GFP) of MVP. The subcellular distribution of the GFP fusion protein expressed in the non-small cell lung carcinoma cell line SW1573 was examined by fluorescence microscopy. A particulate MVP-GFP fluorescence was distributed through the cytoplasm with a denser staining in the perinuclear region (Fig. 1A,a). The fluorescent pattern was similar to the localization of MVP in untransfected cells as detected by immunofluorescence using a mouse monoclonal anti-MVP (Fig. 1A,b). Incubation using an isotype control antibody confirmed the specificity of the fluorescent signal (data not shown). To verify whether the expressed GFP fusion protein is actually incorporated into intact vault particles, we used differential centrifugation. Vault particles have enough mass to be pelleted from a crude cell lysate in a 100,000 ***g*** centrifugation step. The GFP fusion protein was partly recovered in the 100,000 ***g*** pellet fraction, together with endogenous MVP (Fig. 1B). The ratio of GFP-tagged MVP versus endogenous MVP in the pellet (P) fraction reflects their expression levels as determined in the total lysate (TL), indicating that both proteins are equivalent in competing for incorporation into vault particles. Nevertheless, about 35-40% of both the endogenous and GFP-tagged MVP is found in the supernatant fraction. Similarly, on fractionation of SW1573 cells, part of the MVP (10-15%) was recovered in the supernatant (S). The recovery of MVP and MVP-GFP in the supernatant fraction may reflect the in vivo situation in which a portion of the MVP is not incorporated into complexes large enough to be pelleted at 100,000 ***g***. Alternatively, it might be a fractionation artifact. To ascertain that the MVP-GFP is incorporated into genuine vaults, we performed an immunoprecipitation with a rabbit polyclonal anti-GFP antiserum. The subsequent analysis of the immunoprecipitates by immunoblotting showed that the minor vault protein VPARP is associated with the vaults containing MVP-GFP (Fig. 1C).

Dynamics of the vault complex measured by FRAP

We examined vault dynamics in living SW1573 cells expressing MVP-GFP using fluorescence recovery after photobleaching (FRAP). In a FRAP assay specifically suited for determination of effective diffusion coefficients (D_{eff}), we compared the mobility of MVP-GFP (vaults) with that of free GFP. As a control we used a SW1573 transfectant expressing a GFP-tagged deletion mutant of MVP (MVP706-GFP) that is

not incorporated into vault particles, as shown by biochemical fractionation (Fig. 1B).

In the cytoplasm a narrow strip (2 μm) was bleached by a short laser pulse (200 milliseconds) at high laser intensity, after which recovery of the fluorescent signal in the strip was determined at intervals of 100 milliseconds. We observed a full recovery of both GFP and MVP-GFP fluorescence, indicating that all MVP-GFP, whether incorporated into vaults or not, is mobile (Fig. 2A). The diffusion coefficients were calculated from these measurements by least square fitting to curves from computer simulations in which diffusion, bound fraction and residence time were varied (see Materials and Methods) (Hoogstraten et al., 2002). GFP molecules fitted best to a model where all molecules were mobile and had a D_{eff} of 14±2.4 μm^2/s. The MVP-GFP data also fitted best to a model where no bound fraction was present, and with a D_{eff} of 2±0.4 μm^2/s the MVP-GFP molecules were much slower than free GFP. Using the effective diffusion coefficient of GFP determined in our experimental set-up, we estimated that a complex of 10-13 MDa will have a diffusion coefficient of approximately 2 μm^2/s. Therefore, we conclude that in vivo most of the MVP-GFP molecules are incorporated into vault particles. The effective diffusion coefficient of the mutant MVP molecules (MVP706-GFP of about 107 kDa) as determined by least square fitting to the computer simulation curves was ~13 μm^2/s. This value is close to that of free GFP, confirming the fact that the MVP706-GFP molecules are not incorporated into larger complexes. To check whether vault movement was dependent on temperature, FRAP measurements were performed at 37°C and 28°C. A relatively small decrease in temperature (from 310 K to 301 K) has been shown to have little effect on diffusion in living cells (Hoogstraten et al., 2002; Phair and Misteli, 2000; Politz et al., 1999). We observed no significant difference in vault mobility in three independent experiments (Fig. 2B). These results indicate that most of the vaults are freely mobile and move by diffusion.

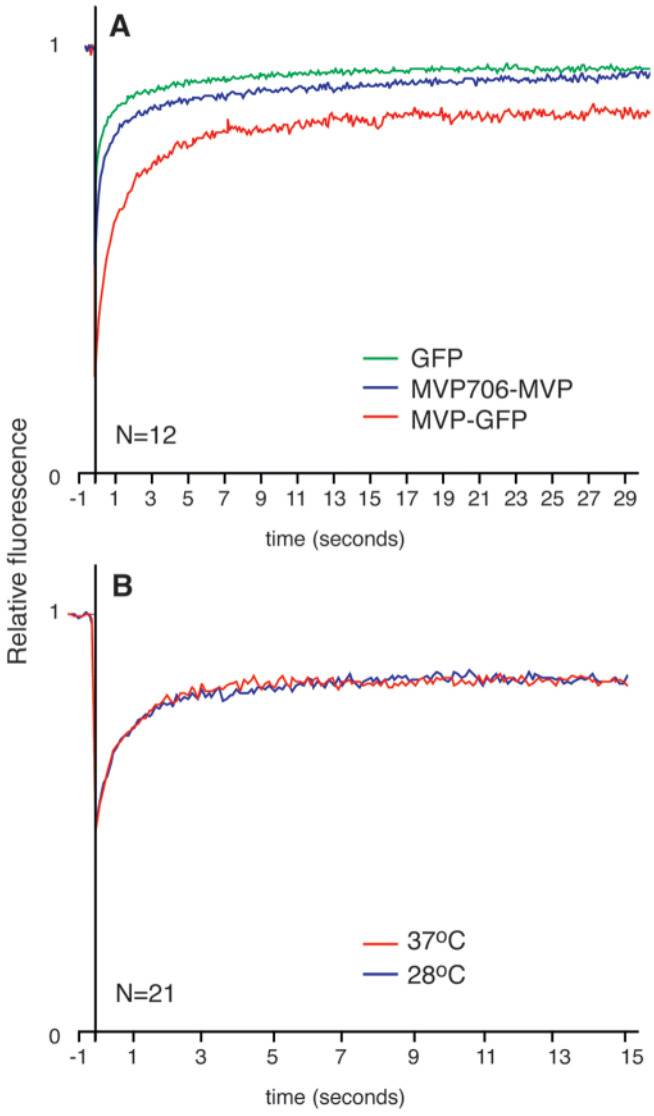

Fig. 2. Dynamics of the vault complex measured by FRAP. (A) The graph shows the mobility of fluorescent MVP-GFP (red line) compared with free GFP (green line) and a GFP-tagged truncated MVP that is not incorporated into vaults (MVP706-GFP, blue line), each measured in 12 cells. Fluorescence intensity before the bleach pulse was set at 1. Note that the recovery of fluorescence is never 100% because of removal of fluorescence by the bleach pulse. This effect differs between proteins depending on their residence time in the strip during bleaching. (B) The redistribution of fluorescent MVP-GFP within a bleached strip was monitored at 37°C (red line) and at 28°C (blue line) with intervals of 100 milliseconds. The graph depicts the data of an experiment in which 21 cells were measured.

Redistribution of MVP-GFP into tube-like structures

Although the diffusion of vaults was not affected at 28°C, we noticed a typical and highly consistent redistribution of the MVP-GFP fluorescence when the transfected cells were incubated at 21°C (room temperature). The characteristic particulate fluorescent pattern observed in cells expressing MVP-GFP cultured at 37°C is shown (Fig. 3A,a and Fig. 1A,a). Incubation of these cells at 21°C for 30-60 minutes resulted in the appearance of elongated fluorescent structures, resembling tubes (Fig. 3A,d). These vault-tubes appeared in 50-80% of the cells and disappeared within 30 minutes when the temperature was raised to 37°C (Fig. 3A,g). Degrading vault-tubes seemed to break open along their longitudinal axis, forming curled sheets, which eventually dissolved to give rise to the regular vault fluorescent pattern (data not shown). When SW1573/MVP-GFP cells were stained for the minor vault protein VPARP (Fig. 3A,b), the fluorescent pattern only partly overlapped with the MVP-GFP fluorescence (Fig. 3A,c). In addition to the fine particulate staining that colocalizes with MVP-GFP, VPARP is also present in the nucleus and in distinct elongated structures. These VPARP-rods are predominantly, but not exclusively, present in the perinuclear region (Fig. 3A,b).

When vault-tubes were allowed to form at 21°C, most of the cytoplasmic VPARP-rods could no longer be detected separately from the MVP-GFP fluorescence (Fig. 3A, e and f). This indicates that the VPARP molecules of the rods are either incorporated in the vault-tubes or that the tubes are formed at the site of the VPARP-rods. By incubating cells at 21°C for a short time (10 minutes) we were able to detect interactions between the VPARP-rods and clusters of MVP-GFP molecules (Fig. 3B). Vault-tubes were not yet formed, but an

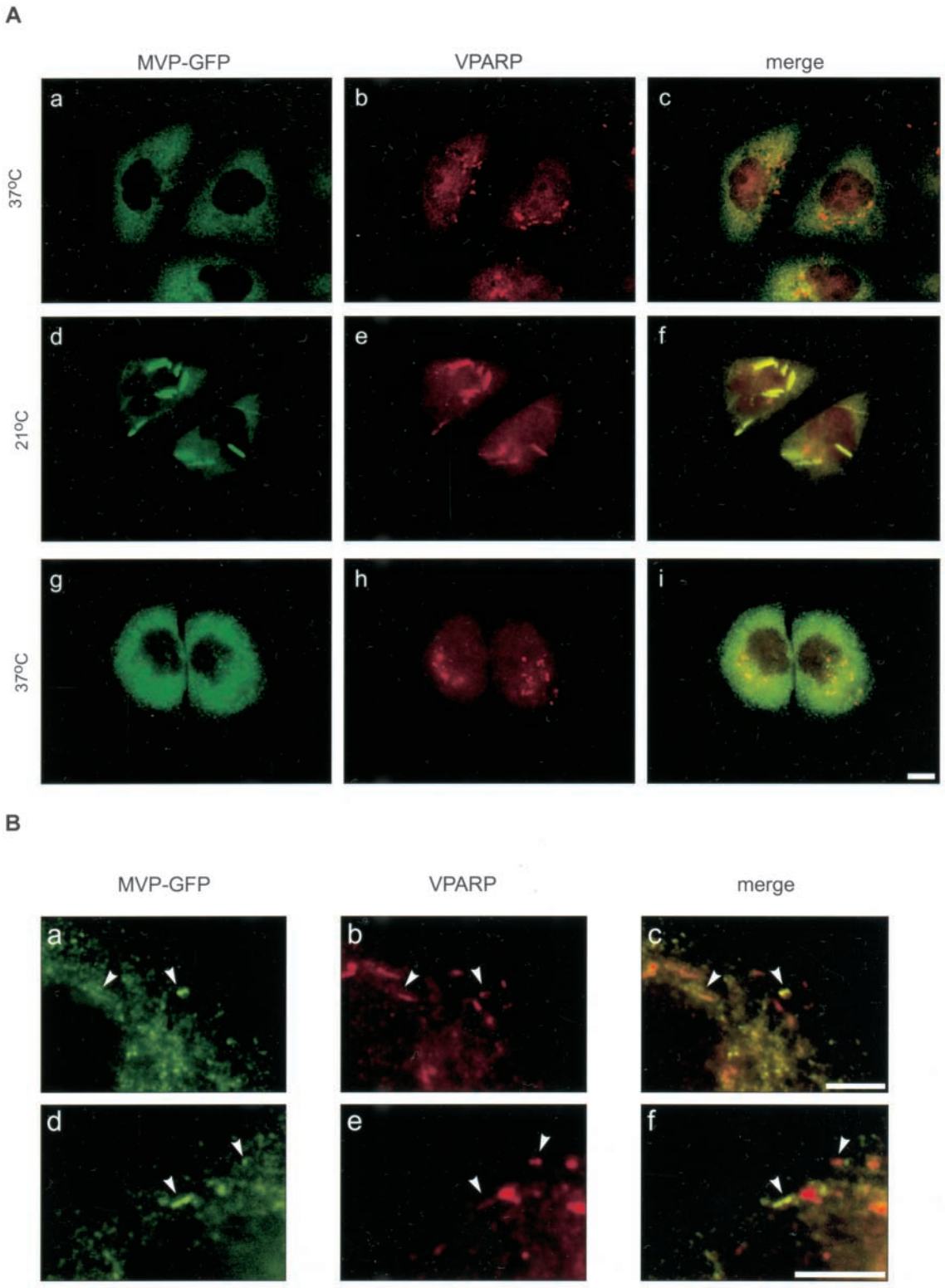

Fig. 3. Formation of vault-tubes. (A) SW1573/MVP-GFP cells were incubated at 37°C (a-c), at 21°C for 60 minutes (d-f) and at 37°C for 30 minutes after the treatment at 21°C (g-i). Shown is the MVP-GFP fluorescent signal (a,d,g), the indirect immunofluorescence staining for VPARP (b,e,h) and the merged images (c,f,i). Incubation at 21°C resulted in the formation of large cytoplasmic, tube-like structures (vault-tubes, d). Under the same conditions VPARP staining reveals a dramatic decrease in the number of non-vault-associated VPARP-rods. The VPARP signal almost completely colocalizes with the tube structures (e and f). Both the MVP and VPARP distribution returns to normal when the cells cultured at 21°C were placed at 37°C for 30 minutes (g-i). Bar, 10 μm. (B) Partial colocalization of GFP-tagged MVP (a and d) and the VPARP-rods (b and e) in the merged picture (c and f) after incubation of SW1573/MVP-GFP cells at 21°C for 10 minutes. The arrowheads point to sites where MVP-GFP clusters have formed, which are in close proximity to the VPARP-rods. Bars, 5 μm.

accumulation of GFP-tagged MVP at the VPARP-rods was observed (Fig. 3B). This implies a recruitment of MVP-GFP (or vaults) to the VPARP-rods, which eventually may lead to vault-tubes. Restoring the temperature to 37°C not only led to the disintegration of the vault-tubes, but also to the reappearance of the non-vault-associated VPARP-rods (Fig. 3A, h and i).

The subcellular localization of VPARP

We verified the presence of VPARP-rods in different – nontransfected – cell lines. A similar subcellular distribution of VPARP – a diffuse localization in both the nucleus and cytoplasm and the presence of cytoplasmic VPARP-rods – was observed in the nontransfected SW1573 and HeLa cells (Fig. 4A, a and b), as well as in the drug-resistant SW1573/2R120 and African green monkey kidney (COS) cells (data not shown). The specificity of the VPARP staining was confirmed by the absence of fluorescent signal when an isotype control was used (Fig. 4A,c). The length of the VPARP-rods differed in a cell-line-dependent manner. In particular, the differences in length between the parental SW1573 and the MVP-GFP transfected SW1573 pointed to a correlation between MVP expression levels and the length of the VPARP-rods. We therefore measured VPARP-rod length in SW1573 cells, its drug-resistant, vault-overexpressing derivative SW1573/2R120 and the SW1573/MVP-GFP transfectant. The average length varied from 1.5 μm in SW1573/MVP-GFP to 2.3 μm in SW1573 cells (Fig. 4B, left-hand graph). Although the orientation of the VPARP-rods may vary, the differences in length were significant (P<0.05), confirming our visual observations. The length of the VPARP-rods may have differed because of the differences in the expression level of VPARP. Nevertheless, western blot analysis indicated that the total levels of expressed VPARP were similar in these cell lines (Fig. 4B, right-hand graph). As expected, MVP was upregulated in the drug-resistant cells (usually around 1.5-fold compared with the parental SW1573 cell line) and in the MVP-GFP-transfectant cells (almost threefold). The size of the cytoplasmic VPARP-rods appeared to inversely correlate with the MVP expression levels.

The coiled-coil domain of MVP is necessary for vault-tube formation

To exclude the possibility that the occurrence of vault-tubes at 21°C is due to overexpression of MVP-GFP or the addition of the GFP-tag, the formation of vault-tubes was investigated in SW1573/2R120 and parental, nontransfected SW1573 cells (Fig. 5A). Vault-tubes, detected by indirect immunofluorescence, were observed in both cell lines, indicating that they are not caused by the overexpression of GFP-tagged MVP. To test whether MVP-MVP interactions are necessary for vault-tube formation we used the stable SW1573 transfectant expressing a GFP-tagged deletion mutant of MVP. The MVP is truncated at its C-terminal end, resulting in a partial deletion of the coiled-coil domain (MVP706-GFP). The coiled-coil domain at the C-terminal half of MVP is essential for the interaction of MVP molecules and consequently for the assembly of vault particles (van Zon et al., 2002). The deletion mutant is unable to interact with other MVP molecules and is not incorporated into vault particles (Fig. 1B, Fig. 2A) (van

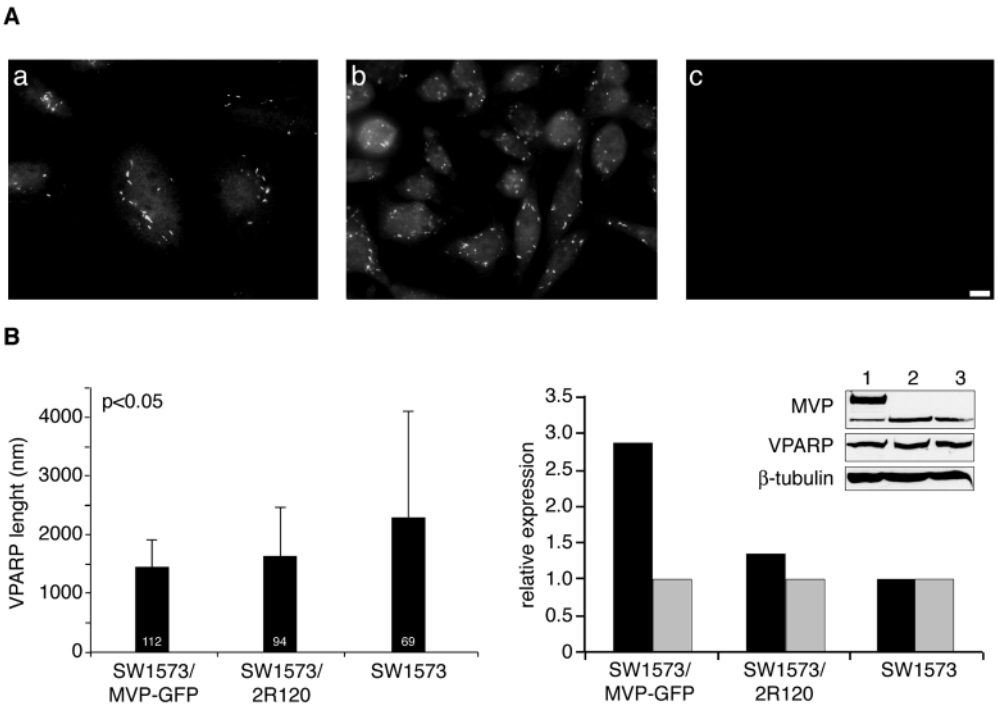

Fig. 4. Cytoplasmic VPARP-rods and their relation to MVP expression levels. (A) Anti-VPARP staining of untransfected SW1573 (a) and HeLa (b) cells showed a normal VPARP distribution, including the VPARP-rods. Background staining was absent as revealed by the staining of SW1573 cells with an isotype antibody (c). Bar, 10 μm. (B) The left-hand graph depicts the average length of the VPARP-rods in untransfected SW1573 cells, in its vault-overexpressing drug-resistant derivative SW1573/2R120 and in the SW1573/MVP-GFP transfectant. The numbers in the bars indicate the number of VPARP-rods measured. The data were analyzed by the Student's *t*-test. The P-value was in all cases below 0.05, indicating statistically significant differences. The right-hand graph shows the quantification of the MVP (black bars) and VPARP (gray bars) levels as determined by immunoblotting (see inlay; lane 1, SW1573/MVP-GFP; lane 2, SW1573/2R120; and lane 3, SW1573, with equal amounts of total protein loaded). The levels of VPARP and MVP in the SW1573 cells are arbitrarily set at 1 and corrected for loading using the β-tubulin signal as a reference. Note that the two protein bands visible in the MVP panel in lane 1 represent the endogenous MVP and the MVP-GFP fusion product.

Zon et al., 2002). Expression of the truncated fusion protein resulted in a less particulate, more diffuse fluorescent staining pattern compared with the full-length MVP-GFP (Fig. 5B, a and b). Incubation at 21°C led to the formation of GFP-labeled vault-tubes in control cells, but not in the coiled-coil mutant (Fig. 5B, c and d). This indicates that MVP molecules have to interact with each other via their coiled-coil domain in order to form vault-tubes. It is therefore probable that vault-tubes contain intact vaults.

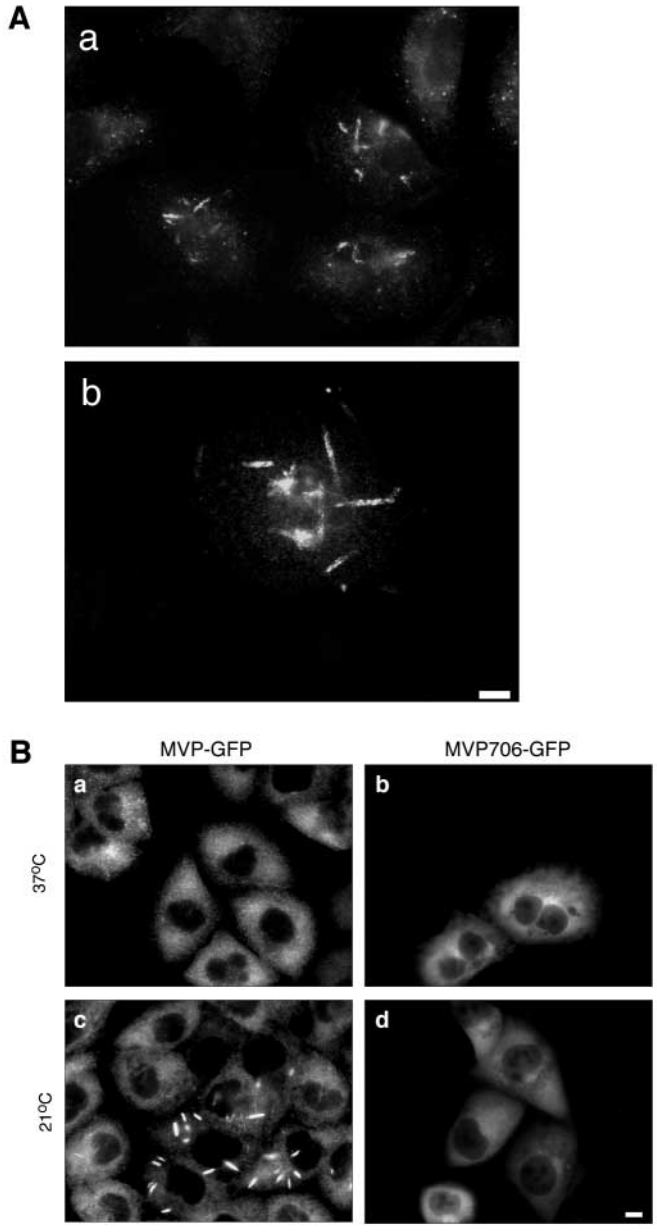

Fig. 5. Coiled-coil domain of MVP essential for incorporation into vault-tubes. (A) Vault-tube formation, by a 60 minute incubation at 21°C, could be observed in nontransfected SW1573 (a) and SW1573/2R120 (b) cells immunodetected with anti-MVP (LRP-56 mAb). Bar, 10 μm. (B) Stably transfected SW1573 cells expressing either full-length MVP (a and c) or the amino acids 1-706 of MVP (b and d) fused to GFP were incubated at 21°C for 60 minutes. The GFP-tagged proteins in which a part of the coiled-coil domain of MVP is deleted (MVP706-GFP) are not incorporated into vault-tubes. Bar, 10 μm.

Dimensions and dynamics of the vault-tubes

Confocal microscopy revealed that vault-tubes, which are formed at 21°C, are cylinders with highly regular dimensions (Fig. 6A). In living SW1573/MVP-GFP cells, the vault-tubes had an average length of 7±2 μm (range 4.5-12 μm; n=16) and a width of 1.5±0.3 μm (n=18). To study whether vault-tubes are stable or dynamic structures (where MVP molecules bind and release frequently), we performed FRAP experiments on these structures (Fig. 6B). Surprisingly, approximately 100 seconds after the laser pulse the fluorescence in the bleached area had completely recovered, indicating that the vault-tubes are dynamic structures in which individual MVP molecules have residence times of on average 100 seconds. Attempts to quantify the fluorescent redistribution were hampered by the fact that the vault-tubes are relatively narrow and tend to move, leading to inaccurate measurements. In the current experimental set-up we could not determine whether the observed exchange of fluorescence was the result of individual MVP-GFP molecules moving to and from vault-tubes or whether it represented the exchange of whole vault particles.

Integrity of microtubules affects vault-tube formation

Vaults have been suggested to function in cytoplasmic transport, possibly via the microtubules (Hamill and Suprenant, 1997; Herrmann et al., 1999). The question arises as to what extent the microtubules are involved in the vault-tube formation. There are no visible differences in the β-tubulin staining in cells cultured at 37°C and 21°C, indicating no dramatic effects on the microtubules when the temperature drops to 21°C. To investigate whether microtubule destabilization or stabilization results in vault-tube formation, we treated SW1573/MVP-GFP cells with either 30 μM nocodazole or 20 μM taxol for 60 minutes (Fig. 7). The depolymerization of microtubules by nocodazole did not result in vault-tube formation at 37°C, nor did the taxol incubation, which stabilizes microtubules. However, when the treated cells were incubated at 21°C for 60 minutes clear differences in the amount of cells with vault-tubes were observed. Vault-tubes were observed in approximately 80% (n=608) of the nocodazole-treated cells. By contrast, 60% (n=684) of the control cells contained vault-tubes, whereas only 3% (n=645) of the taxol-treated cells showed vault-tube formation. Apparently, the stability of the microtubules plays a significant role in tube formation at 21°C. However, destabilization or stabilization alone is not sufficient to initiate vault-tube assembly at 37°C.

Discussion

Vaults are large ribonucleoprotein particles that may play a role in intracellular transport; however, their precise cellular function is unknown. Here, we investigated the dynamics and subcellular distribution of vaults using GFP-tagged MVP molecules expressed in non-small cell lung carcinoma cells. All experiments shown were performed with SW1573 cells expressing a C-terminal tagged MVP; however, identical

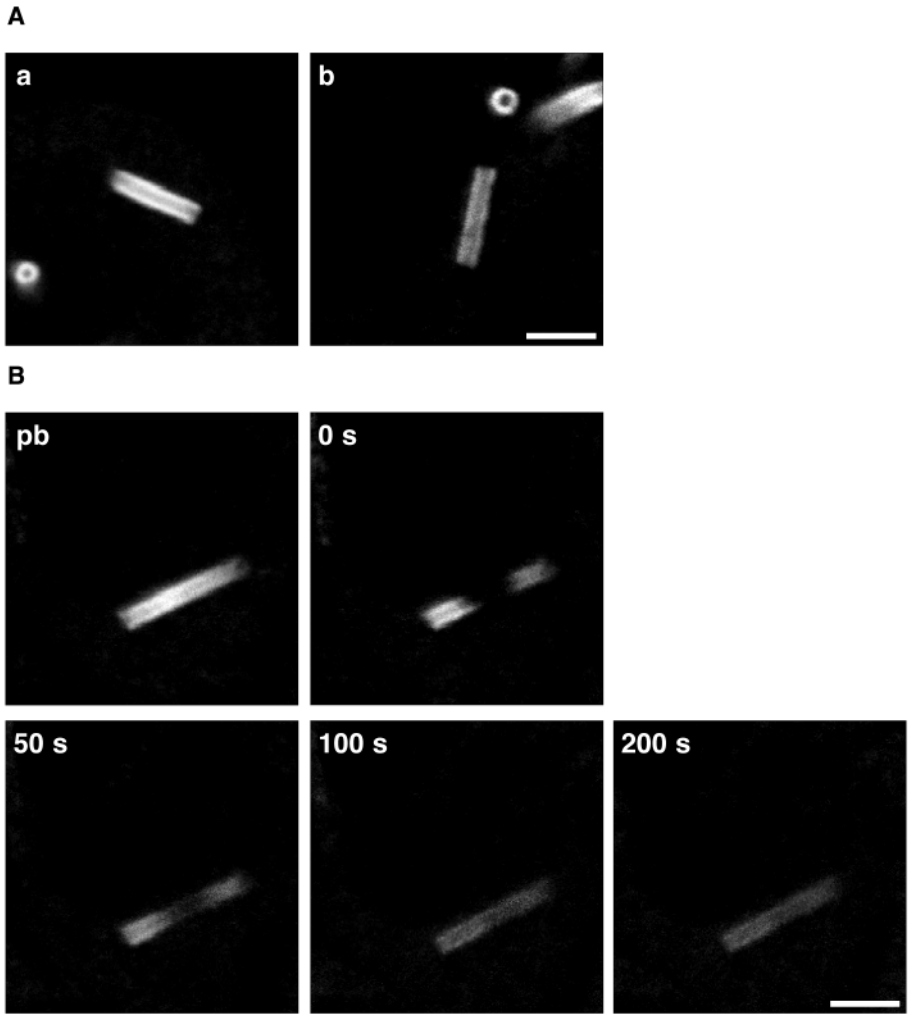

Fig. 6. Dimensions and dynamics of the vault-tubes. (A) Images obtained by confocal laser scan microscopy on living SW1573/MVP-GFP cells cultured at 21°C clearly show that vault-tubes are hollow cylinders. Depicted are transverse and longitudinal optical sections of the vault-tubes. Bar, 5 μm. (B) Dynamics of the vault-tubes were studied with FRAP. Shown are images from a representative FRAP experiment of a vault-tube before the bleach pulse (pb), directly after bleaching (0 s) and 50, 100 and 200 seconds after the bleach pulse. The rapid recovery of fluorescent staining in the bleached area indicated that vault-tubes are dynamic structures. Bar, 5 μm.

results were found using an N-terminal-tagged MVP fusion protein. Clearly, the outcome of the experiments was not affected by the position of the GFP-tag. At room temperature (21°C), we observed extensive rearrangements in vault distribution and dynamics leading to the formation of vault-tubes. Individual MVP molecules had to interact with each other in order to form the vault-tubes, and the non-vault bound VPARP pool is used during the vault-tube formation. We

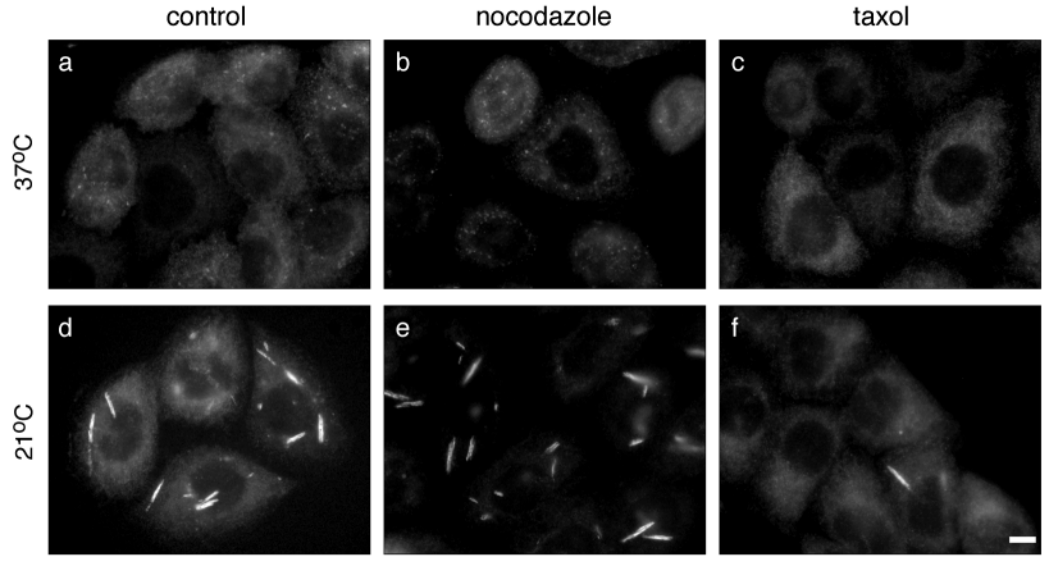

Fig. 7. Vault-tube formation and the stability of microtubules. SW1573/MVP-GFP cells were cultured at 37°C for 60 minutes in the absence (a and d) or presence of 30 μM nocodazole (b and e) or 20 μM taxol (c and f). Subsequently, the cells were placed at 21°C for 60 minutes and monitored for vault-tube formation by fluorescence microscopy. Bar, 10 μm.

therefore believe that complete vault particles are incorporated into the vault-tubes – a process that is completely reversible.

Most of our studies were performed with SW1573 cells expressing MVP tagged with GFP. Therefore, we verified that these tagged proteins are incorporated into genuine vaults. The subcellular localization and appearance of the MVP-GFP fluorescence is similar to the MVP pattern observed in immunostained untransfected cells. Like regular vaults, the GFP-tagged vaults can be precipitated by centrifugation at 100,000 ***g***. These biochemical fractionation data show an equal ratio of MVP and MVP-GFP in the pellet fraction compared with the total lysate. This indicates that both proteins are equivalent in competing for incorporation or assembly. In both the parental and the MVP-GFP-overexpressing cell line we found a fraction of MVP/MVP-GFP in the supernatant after centrifugation. This might be an artifact of the biochemical fractionation or it may represent an in vivo situation in which not all MVP molecules are incorporated into vault particles. Evidence that MVP-GFP molecules are incorporated into vault particles came from the in vivo FRAP measurements. Although it is likely that the cytoplasmic organization (e.g. cytoskeleton, endoplasmic reticulum) affects vaults kinetics, our data indicated that the majority of MVP-GFP moved as free 10-13 MDa complexes. However, owing to the limited resolution of the microscopic methods used, we cannot completely rule out the possibility that a small fraction behaves differently. The effective diffusion coefficient of the expressed MVP-GFP was similar to the one predicted for vault complexes (see Results section), indicating that in vivo the majority of MVP-GFP is incorporated into vault particles.

The intracellular localization of VPARP only partly overlapped with that of MVP. Unlike vaults, VPARP is present in the nucleus and in elongated structures in the cytoplasm (VPARP-rods). In line with TEP1, which is a shared protein with the telomerase complex (Kickhoefer et al., 1999b), the non-vault-associated VPARP may have separate functions independent of the vault complex. Nevertheless, our results indicate a dynamic link between the non-vault-associated VPARP fraction and vault particles. First, the length of the VPARP-rod seems to be inversely correlated with the MVP expression levels. Relatively high MVP expression levels associate with short VPARP-rods. When more MVP is present in a cell, more vault particles are formed (Siva et al., 2001; Stephen et al., 2001) and probably more VPARP is incorporated into these vaults. Consequently, less non-vault bound VPARP is present in the cell, leading to shorter VPARP-rods. Second, when vault-tubes are allowed to form at 21°C, the VPARP-rods can no longer be detected separately from the tubes. Probably, the VPARP is temporarily incorporated in the vault-tubes. Both the localization of vaults and the VPARP-rods are reversed when the cells are again incubated at 37°C. Finally, we could detect clustering of MVP-GFP on the VPARP-rods when cells were incubated at 21°C for a short time. This indicated the existence of a true physical interaction between MPF-GFP molecules (or vaults) and the VPARP-rods.

An intriguing question concerns the nature of the cytoplasmic VPARP-rods. In a yeast-based two-hybrid system, we showed previously that VPARP is not able to interact with itself (van Zon et al., 2002). Therefore, VPARP-rods probably need other proteins or structures to sustain themselves. The VPARP-rods are relatively small (2 μm × 0.5 μm) compared with the large vault-tubes (7 μm × 1.5 μm). Assuming that the vault-tube is completely covered with vaults in a standing position, one could calculate that there will be around 7500 vault particles per micrometer of vault-tube. Probably, the symmetrical vault itself determines the morphology of the vault-tubes. It was observed in vitro that vaults are able to aggregate side-to-side in large pseudo-crystalline arrays (Kedersha et al., 1991). We showed clustering of vault particles in vivo, indicating that this might be a natural ability of the vault particles.

Because vault particles have been associated with intracellular transport, a function in which the microtubules may participate, we studied the involvement of the microtubules in the vault-tube formation. One scenario might be that the microtubules are damaged by the incubation at room temperature and that this may cause the vault-tubes to form, but depolymerization of the microtubules at 37°C did not result in vault-tubes. However, when the cells were incubated at room temperature, depolymerized microtubules had a stimulating effect on vault-tube formation, and stabilization of the microtubules had an inhibiting effect. The microtubule stability plays a role in the vault-tube formation; however, other impulses are necessary to initiate vault-tube assembly. Lowering of the temperature also affects the efficiency of enzymatic reactions and may influence protein conformation. Preliminary results showed that small vault-tubes appear when cells cultured at 37°C are treated with PARP-inhibitors, like 3-aminobenzamide or DPQ [3,4-dihydro-5-[4-(1-piperidinyl) butoxy]-1(2*H*)-isoquinoline], which suggests that the inhibition of the enzymatic activity of VPARP may play a role in tube formation. Although these results are interesting, also the VPARP activity appears to be a small element in the complex event of the vault-tube formation.

This work was supported by a grant to EACW from the Dutch Organization for Scientific Research (NWO, 902-21-213).

References

Abbondanza, C., Rossi, V., Roscigno, A., Gallo, L., Belsito, A., Piluso, G., Medici, N., Nigro, V., Molinari, A. M., Moncharmont, B. et al. (1998). Interaction of vault particles with estrogen receptor in the MCF-7 breast cancer cell. *J. Cell Biol.* **141**, 1301-1310.

Chugani, D. C., Rome, L. H. and Kedersha, N. L. (1993). Evidence that vault ribonucleoprotein particles localize to the nuclear pore complex. *J. Cell Sci.* **106**, 23-29.

D'Amours, D., Desnoyers, S., D'Silva, I. and Poirier, G. G. (1999). Poly(ADP-ribosyl)ation reactions in the regulation of nuclear functions. *Biochem. J.* **342**, 249-268.

Hamill, D. R. and Suprenant, K. A. (1997). Characterization of the sea urchin major vault protein: a possible role for vault ribonucleoprotein particles in nucleocytoplasmic transport. *Dev. Biol.* **190**, 117-128.

Harrington, L., McPhail, T., Mar, V., Zhou, W., Oulton, R., Bass, M. B., Arruda, I. and Robinson, M. O. (1997). A mammalian telomerase-associated protein [see comments]. *Science* **275**, 973-977.

Herrmann, C., Volknandt, W., Wittich, B., Kellner, R. and Zimmermann, H. (1996). The major vault protein (MVP100) is contained in cholinergic nerve terminals of electric ray electric organ. *J. Biol. Chem.* **271**, 13908-13915.

Herrmann, C., Golkaramnay, E., Inman, E., Rome, L. and Volknandt, W. (1999). Recombinant major vault protein is targeted to neuritic tips of PC12 cells. *J. Cell Biol.* **144**, 1163-1172.

Hoogstraten, D., Nigg, A. L., Heath, H., Mullenders, L. H., van Driel, R., Hoeijmakers, J. H., Vermeulen, W. and Houtsmuller, A. B. (2002). Rapid

switching of TFIIH between RNA polymerase I and II transcription and DNA repair in vivo. *Mol. Cell* **10**, 1163-1174.

Kedersha, N. L. and Rome, L. H. (1986). Isolation and characterization of a novel ribonucleoprotein particle: large structures contain a single species of small RNA. *J. Cell Biol.* **103**, 699-709.

Kedersha, N. L., Heuser, J. E., Chugani, D. C. and Rome, L. H. (1991). Vaults. III. Vault ribonucleoprotein particles open into flower-like structures with octagonal symmetry. *J. Cell Biol.* **112**, 225-235.

Kickhoefer, V. A., Siva, A. C., Kedersha, N. L., Inman, E. M., Ruland, C., Streuli, M. and Rome, L. H. (1999a). The 193-kD vault protein, VPARP, is a novel poly(ADP-ribose) polymerase. *J. Cell Biol.* **146**, 917-928.

Kickhoefer, V. A., Stephen, A. G., Harrington, L., Robinson, M. O. and Rome, L. H. (1999b). Vaults and telomerase share a common subunit, TEP1. *J. Biol. Chem.* **274**, 32712-32717.

Kickhoefer, V. A., Liu, Y., Kong, L. B., Snow, B. E., Stewart, P. L., Harrington, L. and Rome, L. H. (2001). The telomerase/vault-associated protein TEP1 is required for vault RNA stability and its association with the vault particle. *J. Cell Biol.* **152**, 157-164.

Kitazono, M., Sumizawa, T., Takebayashi, Y., Chen, Z. S., Furukawa, T., Nagayama, S., Tani, A., Takao, S., Aikou, T. and Akiyama, S. (1999). Multidrug resistance and the lung resistance-related protein in human colon carcinoma SW-620 cells [see comments]. *J. Natl. Cancer Inst.* **91**, 1647-1653.

Kitazono, M., Okumura, H., Ikeda, R., Sumizawa, T., Furukawa, T., Nagayama, S., Seto, K., Aikou, T. and Akiyama, S. (2001). Reversal of LRP-associated drug resistance in colon carcinoma SW-620 cells. *Int. J. Cancer* **91**, 126-131.

Kong, L. B., Siva, A. C., Rome, L. H. and Stewart, P. L. (1999). Structure of the vault, a ubiquitous celular component. *Structure Fold. Des.* **7**, 371-379.

Kong, L. B., Siva, A. C., Kickhoefer, V. A., Rome, L. H. and Stewart, P. L. (2000). RNA location and modeling of a WD40 repeat domain within the vault. *RNA* **6**, 890-900.

Kuiper, C. M., Broxterman, H. J., Baas, F., Schuurhuis, G. J., Haisma, H. J., Scheffer, G. L., Lankelma, J. and Pinedo, H. M. (1990). Drug transport variants without P-glycoprotein overexpression from a human squamous lung cancer cell line after selection with doxorubicin. *J. Cell Pharmacol.* **1**, 35-41.

Li, J. Y., Volknandt, W., Dahlstrom, A., Herrmann, C., Blasi, J., Das, B. and Zimmermann, H. (1999). Axonal transport of ribonucleoprotein particles (vaults). *Neuroscience* **91**, 1055-1065.

Parker, B. A. and Stark, G. R. (1979). Regulation of simian virus 40 transcription: sensitive analysis of the RNA species present early in infections by virus or viral DNA. *J. Virol.* **31**, 360-369.

Phair, R. D. and Misteli, T. (2000). High mobility of proteins in the mammalian cell nucleus. *Nature* **404**, 604-609.

Politz, J. C., Tuft, R. A., Pederson, T. and Singer, R. H. (1999). Movement of nuclear poly(A) RNA throughout the interchromatin space in living cells. *Curr. Biol.* **9**, 285-291.

Scheffer, G. L., Schroeijers, A. B., Izquierdo, M. A., Wiemer, E. A. and Scheper, R. J. (2000). Lung resistance-related protein/major vault protein and vaults in multidrug-resistant cancer [In Process Citation]. *Curr. Opin. Oncol.* **12**, 550-556.

Schroeijers, A. B., Siva, A. C., Scheffer, G. L., de Jong, M. C., Bolick, S. C., Dukers, D. F., Slootstra, J. W., Meloen, R. H., Wiemer, E., Kickhoefer, V. A. et al. (2000). The Mr 193,000 vault protein is up-regulated in multidrug-resistant cancer cell lines. *Cancer Res.* **60**, 1104-1110.

Siva, A. C., Raval-Fernandes, S., Stephen, A. G., LaFemina, M. J., Scheper, R. J., Kickhoefer, V. A. and Rome, L. H. (2001). Up-regulation of vaults may be necessary but not sufficient for multidrug resistance. *Int. J. Cancer* **92**, 195-202.

Smith, S. (2001). The world according to PARP. *Trends Biochem. Sci.* **26**, 174-179.

Stephen, A. G., Raval-Fernandes, S., Huynh, T., Torres, M., Kickhoefer, V. A. and Rome, L. H. (2001). Assembly of vault-like particles in insect cells expressing only the major vault protein. *J. Biol. Chem.* **276**, 23217-23220.

van Zon, A., Mossink, M. H., Schoester, M., Scheffer, G. L., Scheper, R. J., Sonneveld, P. and Wiemer, E. A. (2001). Multiple human vault RNAs. Expression and association with the vault complex. *J. Biol. Chem.* **276**, 37715-37721.

van Zon, A., Mossink, M. H., Schoester, M., Scheffer, G. L., Scheper, R. J., Sonneveld, P. and Wiemer, E. A. (2002). Structural domains of vault proteins: a role for the coiled coil domain in vault assembly. *Biochem. Biophys. Res. Commun.* **291**, 535-541.